

Microstructure and wear properties of hardfacing metal manufactured by SMAW with hardfacing electrode adding ferroalloys nitrated jointly

Wonchol Son^A, UnChol Ri^{B*+}, Songgil Jong^A, GumChol Ri^C, HuiChong KANG^B, Wonzun Ri^A, Sokchol Ri^A

^A. Faculty of Materials Engineering, Kimchaek University of Technology, Pyongyang, D P R of Korea

^B. Faculty of renewable Energy Science, HamHung University of Hydraulics and Power, Ham Hung, D P R of Korea

^C. Faculty of Architecture Engineering, HamHung Construction University, Ham Hung, D P R of Korea

*Correspondence: UnChol Ri, HamHung University of Hydraulics and Power, Ham Hung, D P R of Korea

+ E-mail address: riunchol@163.com

ARTICLE INFO

ABSTRACT

Keywords:

Ferroalloy nitriding
Fe-C-Cr, Hardfacing
Microstructure
Wear resistance
SMAW

In order to improve wear resistance of components such as screws with severe friction-wear, microstructure and wear resistance of Fe-C-Cr-Mo-V-Ti-N hardfacing metal were investigated. Ferroalloys added into the coating of hardfacing electrodes were nitrated jointly. The microstructure and wear resistance of hardfacing metals were characterized by means of X-ray diffraction (XRD), optical microscopy (OM), field emission scanning electron microscope (FESEM) and energy dispersive X-ray spectrometry (EDS). In addition, Factsage 7.0 software was used to calculate the equilibrium phase diagram of the hardfacing metals. The results show that the hardfacing layers mainly consist of martensite, austenite, α -Fe, M₂₃C₆, M₇C₃, V₈C₇-type carbides and MX-type complex precipitations (M= V, Ti; X=C, N). The Fe-C-Cr-Mo-V-Ti-N hardfacing layer possesses 1.5 times higher wear resistance than cladding layers without nitrides.

1. Introduction

Fe-based alloy hardfacing electrodes containing different combinations of chromium and carbon are very commonly used in industries [1-3]. In general, wear resistance of the hardfacing layer depends on the combination of hardness and the microstructure. Different alloying elements such as titanium, vanadium, niobium, and molybdenum must be added to improve the microstructure and hardness of Fe-Cr-C hardfacing alloys [4-7]. Carbides of V and Ti have a good thermal stability and the ability to obtain the fine microstructure, and carbide of Mo has been known to be solid solution strengthening and precipitation hardening in the hardfacing metals [8, 9].

Researchers have recently been studying the microstructure and properties of Fe-Cr-C alloys by adding nitrogen. Alloying elements such as Nb, Ti and V are strong carbide-forming elements, and, at the same time, nitride-forming elements [10-14]. Carbonitride precipitation in Fe-Cr-C hardfacing alloys containing nitrogen obviously refines and dispersion-strengthens the matrix to enhance hardness and wear resistance [15, 16]. Meanwhile, the microstructure and abrasive impact wear resistance of high chromium Fe-Cr-C hardfacing alloy, which developed with flux cored wire jointly adding nitrated ferrochromium, ferroniobium and ferrotitanium by an open arc welding,

was investigated [17]. Previous studies showed that the attempts have been made to consider the effect of complex carbonitride precipitates (Ti and Nb) synthesized by metallurgical reaction during SMAW process on microstructure and properties of hardfacing alloys. Here, in hardfacing electrode coating nitrated chromium alloy or nitrated ferrochromium as source of nitride, Fe-Ti and Fe-Nb were introduced. To the best of our knowledge there are no results in the literature regarding the carbonitrides precipitate and wear-out characteristics in hardfacing alloy which is made by electrode with coating containing ferroalloys jointly nitrated without using nitrated chromium alloy or nitrated ferrochromium. The aim of this study is to increase of carbonitride precipitations and enhance wear resistance of hardfacing alloys. A mixed amount of Fe-Ti, Fe-V, Fe-Mo, Fe-Cr and Fe-Mn (The amounts of Fe-V and Fe-Mo are larger than that of Fe-Ti) are jointly nitrated and added in coating of hardfacing electrode. Those are expected to form more amount of carbonitrides. Hardfacing layers were deposited on low carbon steel substrates by shielded manual arc welding (SMAW). The microstructure and wear resistance of hardfacing layers deposited with nitrated ferroalloys was compared with that of hardfacing layers deposited with non-nitrated ferroalloys. The new hardfacing electrode will make the microstructure refined and

wear resistance enhanced, it is helpful to the reproduction of components such as screws under severe friction-wear.

2. Experimental materials and method

Table 1 . Chemical composition of Q235 steel (wt. %).

Element	C	Si	Mn	P	S
Content	≤0.20	≤0.35	≤1.40	≤0.03	≤0.03

Table 2. Chemical composition of ferroalloys (wt. %)

Ferro-Alloy	Cr	Ti	V	Mo	C	Si	P	S
Fe-Cr	60	-	-	-	6.5	3.0	0.07	0.04
Fe-Ti	-	23	-	-	0.2	4.5	0.05	0.06
Fe-V	-	-	60	-	0.7	3.0	0.20	0.10
Fe-Mo	-	-	-	60	0.5	0.8	0.15	1.0

Table 3. Composition of hardfacing electrode coatings (wt. %).

marble	fluorite	feldspar	graphite	Fe-Cr	Fe-V	Fe-Mo	Fe-Ti	Fe-Mn
11	5	3	6	40	15	10	8	2

The ferroalloys for adding into hardfacing electrode coating were nitrided following the steps below. A mixed amount of ferro-alloys (Table 3) was stretched to a thickness of 5 to 7 mm in a container, which was then nitrided in a nitriding furnace. After being heated by 450°C, ammonia gas was injected into the furnace and then maintained at the temperature of 600°C for 10 h. Finally, the furnace was switched off and slow cooled down to 300°C. Subsequently, the nitrogen gas stopped being injected. The slag system is CaO-CaF₂-SiO₂ and the coating includes 25% slag formers and 75% ferroalloys. The outer diameter of the coated

2.1. Experimental materials

The core of hardfacing electrode is Q235 of 5mm in diameter (Table 1). The compositions of ferroalloys and electrode coating are listed in Tables 2 and 3, respectively.

electrode, D, is 7.5mm. Plates of plain carbon steel (Q235) of dimensions 200×100×10mm were used for hardfacing.

2.2. Experimental method

Before hardfacing, the sample was grinded and then cleaned with acetone. The hardfacing electrode was dried at 250°C for 2 h in a drying furnace. Using the manual arc welding method, 5 layers were deposited on each of the specimens in order to obtain homogeneous specimens. The welding parameters and the total thickness of layers are listed in Table 4.

Table 4 . Hardfacing processing parameters.

Current (A)	Voltage (V)	Speed (cm/min)	Layer Thickness (mm)
180~200	20~25	8~10	10

Specimens of dimension 10×10×10 mm were cut off from the middle of hardfacing plate. The specimens were ground using SiC waterproof paper from 200 to 1500 grit, and were then polished with diamond compound polishing paste. The phase structure of hardfacing alloy was analyzed by X-ray diffraction (XRD) of a D/max-2500/PC diffractometer equipped with Cu-K α radiation, with a scanning range of 20° ≤ 2 θ ≤ 80° and a step size of 0.06°, and the dwell time was 2s. After the specimen had been etched with a solution of 5g FeCl₃ +10ml HNO₃+3ml HCl+87ml ethylalcohol, the microstructure was analyzed using an OLYMPUS–DSX500 optical microscope and a ZEISS field emission scanning electron microscope (FESEM). Each phase composition was analyzed by energy dispersive X-ray spectrometry (EDS). Factsage 7.0 (FSstel - FactSage steel database) was used to calculate

the phase diagram of hardfacing metal. Wear test was performed by a MMU-10G pin-on-disk friction and wear testing apparatus at room temperature (20°C). 40Cr steel ring was recommended for wear couple. A pair of 3 cylindrical pin specimens of dimension 4.8×13 mm was tested for 30 min at load of 300N and a rotating speed of 220rpm. The wear resistance of hardfacing layers deposited with nitrided ferroalloys was compared with that of hardfacing layers deposited with non-nitrided ferroalloys. The amount of wear loss was calculated in terms of difference in mass before and after wear-out of the specimen. A basic outline of the pin-on- disc device is given in Fig. 1.

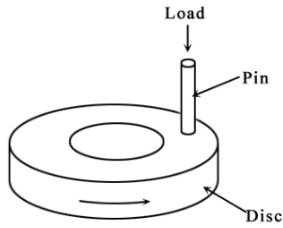


Fig. 1. Sketch of the pin-on-disk.

3. Results and Discussion

3.1. Microstructure and phase structure

The hardfacing layers with nitrated ferroalloys and those with non-nitrated ferroalloys were marked as specimens S1 and S2, respectively. Fig. 1 shows the optical micrograph of the cross-section of specimen S2 hardfacing layer. It indicates good metallurgical bonding between the deposited coating and base metal. The chemical compositions of specimens S1 and S2 are listed in Table 5. They were measured at the top

surface of the hardfacing layers. The result shows that the transition ratio of molybdenum is high. This resulted in a lower affinity of Mo for oxygen compared to those of V and Ti elements.

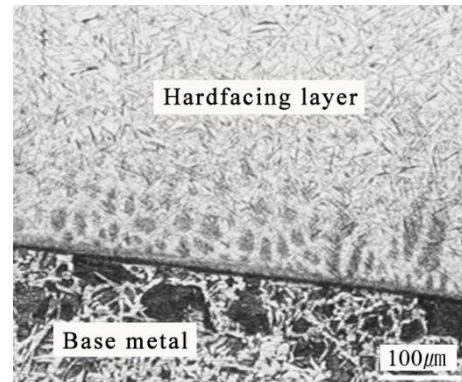


Fig. 2. Cross-sectional optical micrograph of the specimen S2 hardfacing layer.

Table 5. Chemical compositions of hardfacing metals (wt. %).

Specimens	C	Cr	Mo	Mn	Ti	V	N
S1	1.86	12.1	3.1	0.57	0.09	2.25	-
S2	1.84	12.5	3.2	0.58	0.10	2.85	0.28

Figs. 3 and 4 show the optical micrographs (OMs) and XRD results from, the longitudinal sections of specimens S1 and S2, respectively. A hardfacing layer is mainly composed of needle martensite, residual austenite and eutectic phases. Figs. 3 a and 4 a show the dispersed distribution of fine grains with irregular polygonal morphology in the matrix and grain boundaries. These grains can be fined to the size range of 1 to 2 μm . Figs. 3 b and 4 b show that the hardfacing layers of specimens S1 and S2 consisted of $\text{CFe}_{15.1}$ austenite, $\text{C}_{0.05}\text{Fe}_{1.95}$ marten site, α -Fe and M_7C_3 , M_{23}C_6 , V_8C_7 -type carbides. According to the results of XRD, the fine particles in Figs. 3 a and 4 a should be carbides or carbonitrides.

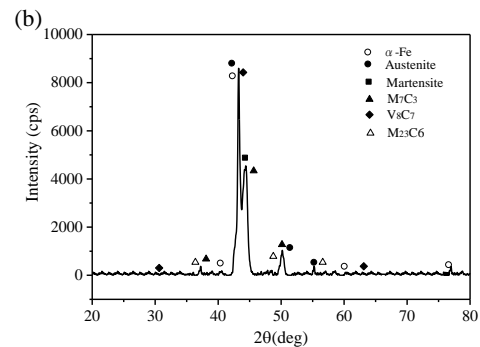
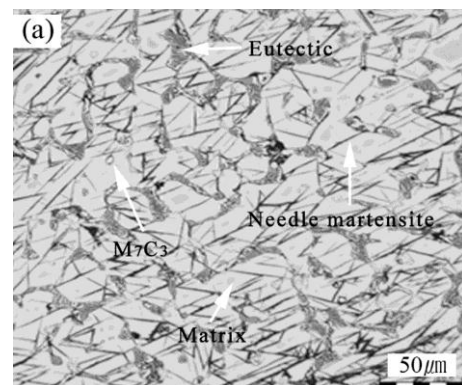
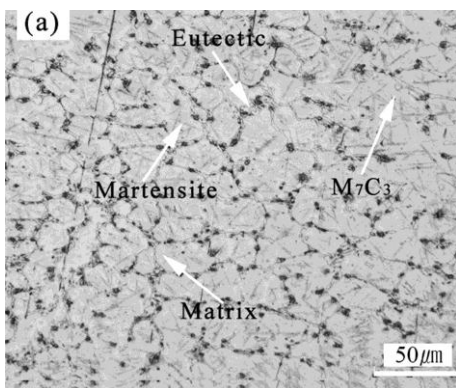


Fig. 3. Microstructure and XRD results of the specimen S1.



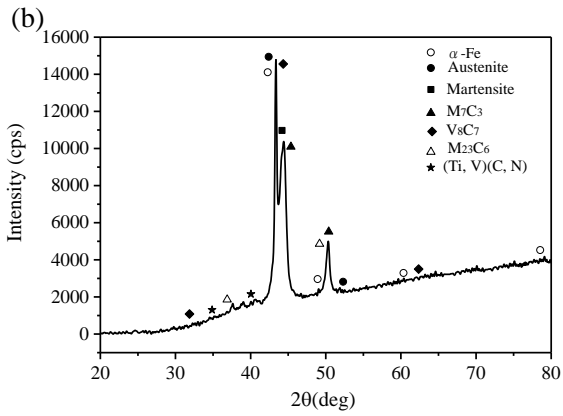
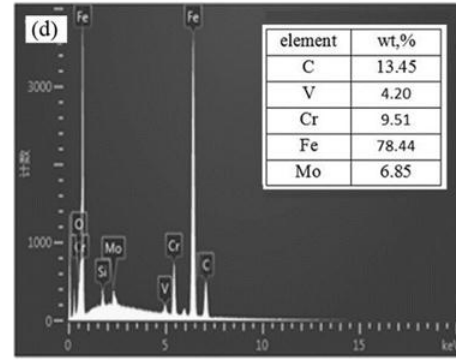


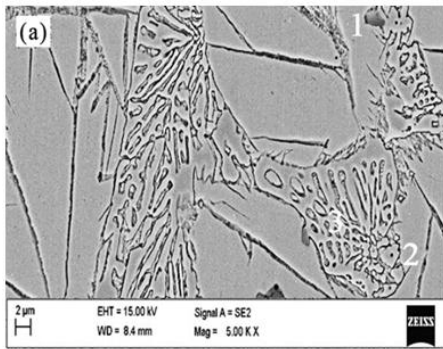
Fig.4. Microstructure and XRD results of the specimen S2.

(c) position 2 in SEM

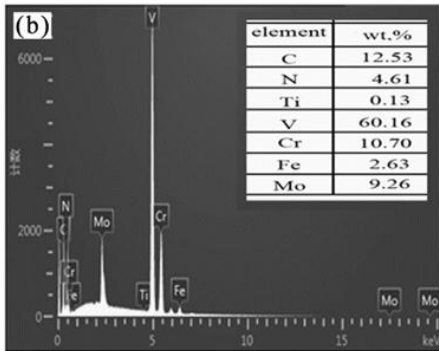


(d) position 3 in SEM

Fig.5. SEM image and EDS results of specimen S2



(a) SEM image



(b) position 1 in SEM

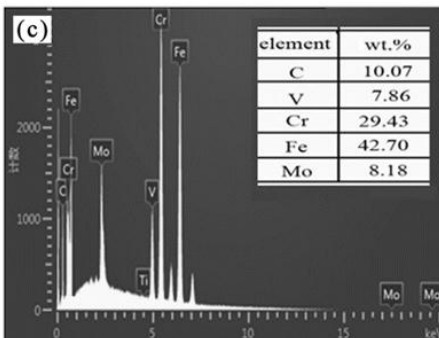


Fig. 5 shows the SEM and EDS results of the longitudinal section of specimen S2. Black particles at position 2 in Fig. 3 a have a lots of vanadium, in which a small amount of Fe, chromium, molybdenum, titanium carbon and nitrogen are contained. As shown in Fig. 5 a, the composition at positions 2 and 3 are identified as chromium, Fe, carbon and vanadium. As shown EDS results in Figs. 4 and 4, it is worth mentioning that the polygonal particles of position 1, 2 and 3 in Fig.5 a are V₈C₇, MX (M=V, Ti; X=C, N)-type carbonitrides, M₇C₃-type carbides and eutectic carbides, respectively. Such complex carbonitrides are well known for high stability and good hot hardness over 600 °C [18].

3.2. Thermodynamic calculation of carbonitrides precipitation

In order to analyze the precipitation rule of the phases in hardfacing layer and the possibility of carbides and carbonitrides forming during the hardfacing solidification process, the equilibrium phase diagram and mass fraction of all solid phases of Fe-C-Cr-Mo-V-Ti-N hardfacing metal were represented (Figs. 6 and 7). The eutectic temperature is located at about 3.7°C. Thus, the microstructure of hardfacing metal with 1.68%C is hypoeutectic.

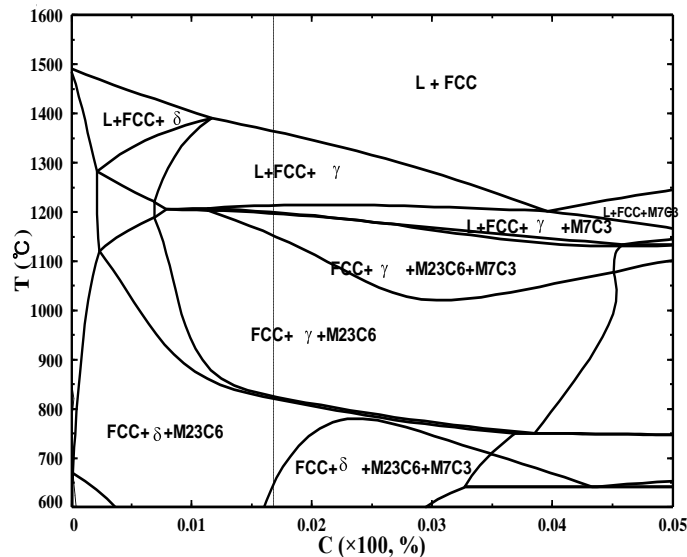


Fig. 6. Equilibrium phase diagram of the Fe-C-Cr-Mo-V-Ti-N hardfacing metal.

Here, as the temperature increases and reaches a peak value at 1360°C, primary austenite is initiated to precipitate. Subsequently, M_7C_3 and $M_{23}C_6$ carbide precipitations occur from the liquid at 1212°C and 1199°C, respectively. Also, δ phase starts to form from the liquid at 822°C.

TiN: 1.25% versus 0.04%. The reason is that the amount of ferrotitanium is less than that of ferrovanadium in ferroalloys of coating, thus, most of ferrotitanium will be exhausted during welding process because titanium has the greater affinity for oxygen than vanadium and molybdenum. Finally, during welding metallurgical reaction process, vanadium-rich carbides or carbonitrides can be formed. It is consistent with the EDS results (Fig. 5 b).

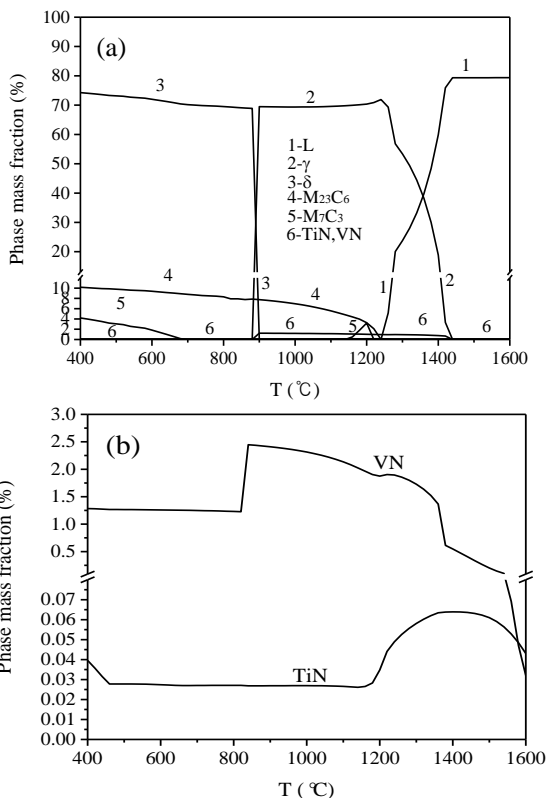


Fig. 7. Mass fraction of solid phases of the specimen S2 hardfacing metal.

3.3. Hardness and wear resistance of hardfacing layers

The hardness of specimens 1 and 2 are listed in Fig. 8. The hardness of S2 was lower than that of S1. This shows that the austenite amount of S2 is comparatively larger than that of S1. The mass losses of specimens S1 and S2 in the atmosphere at 300N, 220r/min, are shown in Fig. 9.

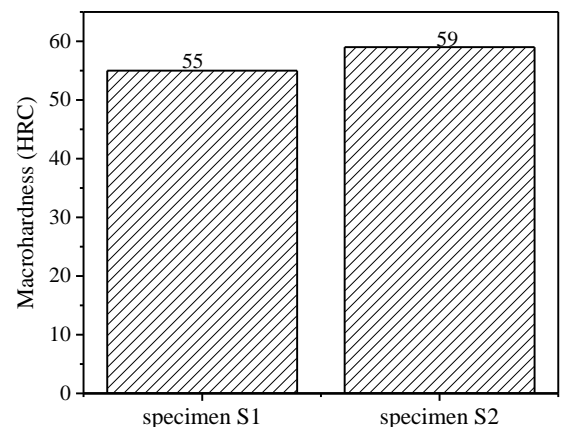


Fig. 8. Macrohardness of specimens S1 and S2.

Meanwhile, from Figs. 6 and 7, it can be confirmed that precipitates with FCC lattice existing in the liquid zone will be nitrides of Ti and V. It shows that the nitrides of Ti and V have already been occurred in the liquid zone. Amount of VN were larger than amount of

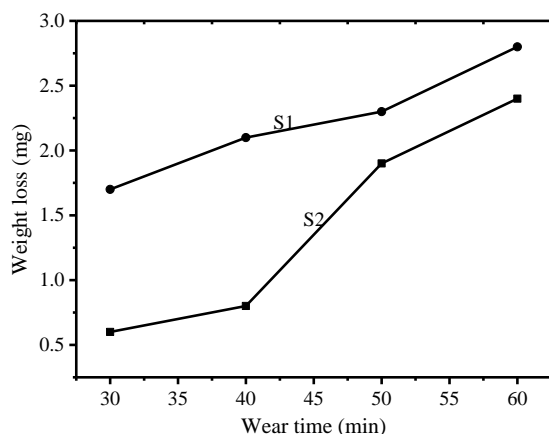
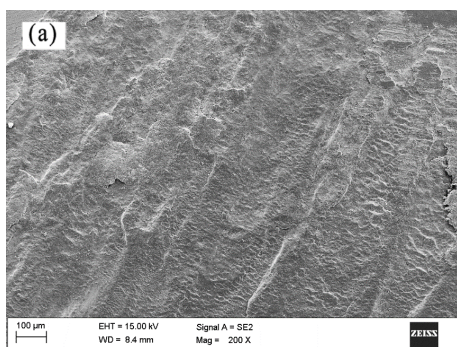
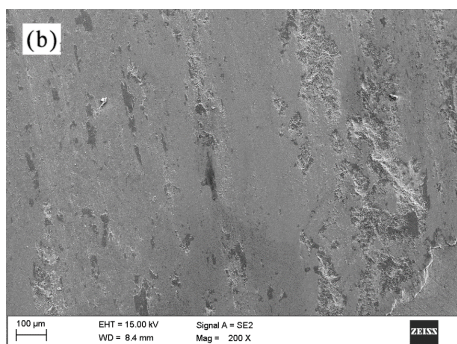


Fig. 9. Wear curve of the hardfacing layers.

Fig. 9 shows that the mass loss of specimen S 2 was lower than that of specimen S 1 in the same conditions. Investigated hardfacing layers consisted of complex carbides and carbonitrides containing V, Mo and Ti. Carbonitrides are distributed homogeneously on the grain boundaries and in the matrix, which contributes to strengthening of hardfacing layers. The carbonitrides have the high temperature stability compared with the carbides [18]. Thus, it helps the wear loss of hardfacing metal to be decreased and the wear resistance to be enhanced. The SEM morphology of the worn surface after the wear test is shown in Fig.10.



(a) specimens S1



(b) specimens S2

Fig.10. Worn morphology of hardfacing metals.

The worn surface of specimen S1 has more roughness than specimen S2, with relatively numerous adhesive craters, deep ploughing grooves, and a lot of detached wear debris, as shown in Fig.10. Compared with hardfacing layers with nitrides, hardfacing layers without nitrides have lower integrity of bonding

between the matrix and carbides. In friction-wear process of hardfacing layers without nitrides, the large carbides are easily exfoliated from the matrix, causing microcutting and microploughing scratches from the matrix.

4. Conclusions

In this paper new approach has been introduced to hardfacing process with ferroalloys nitrided jointly. The following conclusions may be drawn from our findings:

In the ferroalloy nitrided jointly in which ferrovanadium is about 2 times more than ferrotitanium, the amount of vanadium nitrides is larger than that of titanium nitrides. The calculated results of equilibrium phase diagram of Fe-C-Cr-Mo-V-Ti-N alloys show that the nitrides of Ti and V have already been occurred in the liquid zone. Also, amount of VN were larger than amount of TiN: 1.25% versus 0.04%. The complex carbonitrides with rich vanadium concentration is precipitated and disperse-distributed on the grain boundaries and matrix of the hardfacing metal. These are precipitations with size of less than 1~2 μm and tough polygonal morphology. It could be suggested that it is possible to improve the wear resistance of hardfacing metals with nitrides compared to that without nitrides. However, it remains to be further clarified whether our findings could be applied to impact wear. Further studies are needed to determine whether these findings could be applied to components other than those used for friction wear.

Acknowledgements

The authors wish to thank Prof. Gang who gave us much valuable advice in the early stages of this work.

AUTHOR CONTRIBUTIONS

Authors equally contributed.

ORCID

UnChol Ri <http://orcid.org/0000-0002-4474-3389>

Reference

- [1] V.E. Buchanan, D.G. McCartney, P.H. Shipway, A comparison of the abrasive wear behaviour of iron-chromium based hardfaced coatings deposited by SMAW and electric arc spraying, *Wear* 264 (2008) 542–549.
- [2] V.E. Buchanan, P.H. Shipway, D.G. McCartney, Microstructure and abrasive wear behaviour of shielded metal arc welding hardfacing used in the sugarcane industry, *Wear* 263 (2007) 99–110.
- [3] C.P. Tabrett, I.R. Sare, M.R. Ghomashchi, Microstructure-property relationships in high chromium white iron alloys, *Int. Mater. Rev.* 41 (1996) 59–82.
- [4] R.J. Chung, X. Tang, D.Y. Li, B. Hinckley, K. Dolman, Microstructure refinement of hypereutectic high Cr cast irons using hard carbide-forming

- elements for improved wear resistance, *Wear* 301 (2013) 695–706.
- [5] C.-M. Lin, C.-M. Chang, J.-H. Chen, C.-C. Hsieh, W. Wu, Microstructure and wear characteristics of high-carbon Cr-based alloy claddings formed by gas tungsten arc welding (GTAW), *Surface & Coatings Technology* 205 (2010) 2590–2596.
- [6] M. ilipovic, Z. Kamberovic, M. Korac, M. Gavrilovski, Microstructure and mechanical properties of Fe–Cr–C–Nb white cast irons, *Materials and Design* 47 (2013) 41–48.
- [7] C.-M. Lin, C.-M. Chang, J.-H. Chen, W. Wu, The effects of additive elements on the microstructure characteristics and mechanical properties of Cr–Fe–C hardfacing alloys, *Journal of Alloys and Compounds* 498 (2010) 30–36.
- [8] X.W. Qi, Z.N. Jia, Q.X. Yang, Y.L. Yang, Effects of vanadium additive on structure property and tribological performance of high chromium cast iron hardfacing metal, *Surface & Coatings Technology* 205 (2011) 5510–5514.
- [9] X.-H. Wang, F. Han, S.-Y. Qu, Z.-D. Zou, Microstructure of the Fe-based hardfacing layers reinforced by TiC-VC-Mo₂C particles, *Surface & Coatings Technology* 202 (2008) 1502–1509.
- [10] Y. Deng, S.F. Yu, S. Xing, L.B. Huang, Y. Lu, Abrasive resistance of arc sprayed carbonitride alloying self-shielded coatings, *Applied Surface Science* 258 (2011) 382–387.
- [11] K. Yang, X. Xie, R. Zhou, Y. F. Bao, Y. F. Jiang, Study of carbonitride precipitates in the Fe-Cr-Mn-N hardfacing alloy, *Materials Science Forum* 704-705 (2011) 695-699.
- [12] K. Yang, Q. Yang, Y. F. Bao, Effect of carbonitride precipitates on the solid/liquid erosion behaviour of hardfacing alloy, *Applied Surface Science* 284 (2013) 540–544.
- [13] K. Yang, S. F. Yu, Y.B. Li, C.L. Li, Effect of carbonitride precipitates on the abrasive wear behaviour of hardfacing alloy. *Applied Surface Science* 254 (2008) 5023–5027.
- [14] H. S. Ding, S.Q. Liu, H.L. Zhang, J.J. Guo, Improving impact toughness of a high chromium cast iron regarding joint additive of nitrogen and titanium, *Materials and Design* 90 (2016) 958–968.
- [15] K. Yang, Q. Yang, Y. F. Bao, Formation of carbonitride precipitates in hardfacing alloy with niobium addition, *Rare Met.* 32(1) (2013) 52–56.
- [16] S. Z. Wei, Y. Liu, G. S. Zhang, L. J. Xu, J. W. Li, Y. Y. Ren, Microstructure and Wear Resistance of Fe-Cr-C Hardfacing Alloy Reinforced by Titanium Carbonitride, *Tribology Transactions* 58 (2015) 745–749.
- [17] J.B. Wang, T.T. Liu, Y. F. Zhou, X.L. Xing, S. Liu, Y. L. Yang, Q.X. Yang, Effect of nitrogen alloying on the microstructure and abrasive impact wear resistance of Fe-Cr-C-Ti-Nb hardfacing alloy, *Surface and Coatings Technology* 309 (2017) 1072–1080.
- [18] Yogesh Kumar Singla, D.K. Dwivedi, Navneet Arora, On the modeling of dry sliding adhesive wear parameters of vanadium additive iron-based alloys at elevated temperatures, *Surface and Coatings Technology* 283 (2015) 223–233.

Fig. 1. Sketch of the pin-on-disk.

Fig.2. Cross-sectional optical micrograph of the specimen S2 hardfacing layer.

Fig.3. Microstructure and XRD results of the specimen S1.

Fig.4. Microstructure and XRD results of the specimen S2.

Fig.5. SEM image and EDS results of specimen S2;

(a) SEM image (b) position 1 in SEM, (c) position 2 in SEM, (d) position 3 in SEM

Fig.6. Equilibrium phase diagram of the Fe-C-Cr-Mo-V-Ti-N hardfacing metal.

Fig. 7. Mass fraction of solid phases of the specimen S2 hardfacing metal.

(a) mass fraction of all solid phases; (b) mass fraction of nitrides

Fig. 8. Macrohardness of specimens S1 and S2.

Fig. 9. Wear curve of the hardfacing layers.

Fig.10. Worn morphology of hardfacing metals:

(a) specimens S1 (b) specimens S2